2013 European Control Conference (ECC)
July 17-19, 2013, Zürich, Switzerland.

On the Construction of Barrier in a Connectivity Maintenance Game

Sourabh Bhattacharya

Abstract— **In this work, we address the problem of maintaining an operable communication link between two aerial vehicles in the presence of a jammer. This problem was initially proposed in [2]. In this work, we formulate the problem as a game of kind, and present the equations that characterize the barrier in the game using Isaacs' technique [3]. We derive the optimal control of the vehicles on the barrier, and present simulation results for specific terminal conditions.**

I. Introduction

Pursuit-evasion games model situations of conflict that arise between mobile agents. The most common scenario that has been extensively studied in the literature of differential games involves a mobile agent, called a *pursuer*, that tries to capture another mobile agent, called an *evader*. On the contrary, the objective of the evader is to prevent its own capture. In the past, researchers have extended this scenario to teams of mobiles pursuers and evaders involving more than one agent. In [2], the authors introduce a new class of pursuit-evasion problem that involves disruption of the communication channel present within a team of mobile agents due to an intrusion attack inflicted by mobile jammers in the vicinity. This work addresses a similar scenario.

Jamming is a malicious attack whose objective is to disrupt the communication of the victim network intentionally causing interference or collision at the receiver side. Jamming attack is a well-studied and an active area of research in wireless networks. An extensive list of references in jamming attacks relevant to this work is provided in [2]. In the past, we have provided spatial retreat strategies for a team of UAVs trying to establish a communication link in the presence of an aerial jammer in the vicinity [2]. The problem of intrusion evasion was posed as a time optimal zero-sum differential game of degree between the jammer and the team of UAVs. The authors used Isaacs' approach, and performed a regular analysis in order to provide optimal control of the vehicles in the vicinity of termination manifold. In order to complete the construction of the optimal trajectories, the construction of singular surfaces occurring in the game is required, which is in general difficult for games with state space larger than three dimensions. In this work, the stated problem is posed as a game of kind, and the central focus is the construction of the *barrier* that separates the escape set from the capture set. The key concept in the construction of the barrier is that of *semipermeable surfaces*. Once the state of the system is on a semipermeable surface, each player can forbid the other player to cross the surface in a direction favorable to it. In [3], Isaacs showed that the barrier arising in a game of kind possesses the property of semipermeability. In the past, there have been some efforts to compute the barrier, and the associated semipermeable surfaces in games of capture and pursuit. In [13], the authors address collision avoidance strategies for a game with two pursuers and one evader by determining the semipermeable curves that form the barrier. The authors build upon the avoidance strategies for the game of two cars [6], and provide techniques to extend the barrier of the original game in the the presence of an additional pursuer. In [9], the authors provide a description of the semipermeable surfaces appearing in a homicidal chauffeur game and its acoustic modification. The families of semipermeable surfaces are determined only from the dynamics of the system. In [10], the authors further classify the semipermeable surfaces associated with games with "homicidal chauffeur" dynamics based on the roots of the Hamiltonian. In addition to the acoustic version of the homicidal chauffeur game, the authors explore the possibility of distinct semipermeable surfaces for the conic surveillance-evasion problem [5]. In this work, we use Isaacs' approach to construct the barrier from the boundary of the usable part of the terminal manifold. In addition, we provide the optimal strategies for the vehicles once the state of the system is on the barrier.

The organization of the paper is as follows. Section II presents the complete problem formulation. Section III presents the solution technique. Section IV presents the construction of the barrier, and the optimal control of the players along the barrier. Section V presents the simulation results. Section VI presents the conclusions.

II. Communication and Motion Model

In this section, we describe the communication model between two mobile nodes in the presence of a jammer, first introduced in [2]. Then we present the mobility models for the nodes. We conclude the section by formally formulating the problems we study in the paper. The contents of this section have been taken verbatim from Section II of [2], and are presented solely for the sake of reader's convenience.

A. Jammer and Communication Model

Consider a mobile node (*receiver*) receiving messages from another mobile node (*transmitter*) at some frequency. Both communicating nodes are assumed to be lying on a plane. Consider a third node that is attempting to jam the communication channel in between the transmitter and the receiver by sending a high power noise at the same frequency. This kind of jamming is referred to as the *trivial jamming*. A variety of metrics can be used to compare the effectiveness

Sourabh Bhattacharya is with the Mechanical Engineering Department, Iowa State University, Ames, IA 50011 {sbhattac}@iastate.edu

of various jamming attacks. Some of these metrics are energy efficiency, low probability of detection, and strong *denial of service* [8] [7]. In this paper, we use the ratio of the jamming-power to the signal-power (JSR) as the metric. From [11], we have the following models for the JSR (ξ) at the receiver's antenna.

1) R^n model

$$\xi = \frac{P_{J_T} G_{JR} G_{RJ}}{P_T G_{TR} G_{RT}} 10^{n \log_{10}(\frac{D_{TR}}{D_{JR}})}$$

2) Ground Reflection Propagation

$$\xi = \frac{P_{J_T} G_{JR} G_{RJ}}{P_T G_{TR} G_{RT}} (\frac{h_J}{h_T})^2 (\frac{D_{TR}}{D_{JR}})^4$$

3) Nicholson

$$\xi = \frac{P_{J_T} G_{JR} G_{RJ}}{P_T G_{TR} G_{RT}} 10^{4 \log_{10}(\frac{D_{TR}}{D_{JR}})}$$

where P_{J_T} is the power of the jammer transmitting antenna, P_T is the power of the transmitter, G_{TR} is the antenna gain from transmitter to receiver, G_{RT} is the antenna gain from receiver to transmitter, G_{JR} is the antenna gain from jammer to receiver, G_{RJ} is the antenna gain from receiver to jammer, h_J is the height of the jammer antenna above the ground, h_T is the height of the transmitter antenna above the ground, D_{TR} is the Euclidean distance between transmitter and receiver, and D_{JR} is the Euclidean distance between jammer and receiver. All the above models are based on the propagation loss depending on the distance of the jammer and the transmitter from the receiver. In all the above models the jammer to signal ratio is dependent on the ratio $\frac{D_{TR}}{D_{JR}}$.

For digital signals, the jammer's goal is to raise the ratio to a level such that the *bit error rate* [12] is above a certain threshold. For analog voice communication, the goal is to reduce the articulation performance so that the signals are difficult to understand. Hence we assume that the communication channel between a receiver and a transmitter is considered to be jammed in the presence of a jammer if $\xi \geq \xi_{tr}$ where ξ_{tr} is a threshold determined by many factors including application scenario and communication hardware. If all the parameters except the mutual distances between the jammer, transmitter and receiver are kept constant, we can conclude the following from all the above models: If the ratio $\frac{D_{TR}}{D_{JR}} \geq \eta$ then the communication channel between a transmitter and a receiver is considered to be jammed. Here η is a function of ξ, P_{J_T}, P_T, G_{TR}, G_{RT}, G_{JR}, G_{RJ} and D_{TR}. Hence if the transmitter is not within a disc of radius ηD_{JR} centered around the receiver then the communication channel is considered to be jammed. We call this disc as the *perception range*. The *perception range* for any node depends on the distance between the jammer and the node. For effective communication between two nodes, each node should be able to transmit as well as receive messages from the other node. Hence two nodes can communicate if they lie in each other's *perception range*.

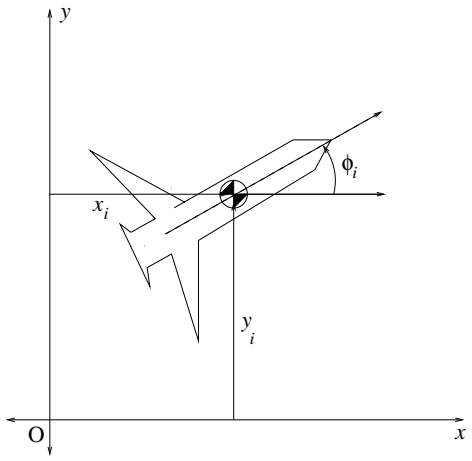

Fig. 1. Configuration of a UAV

B. Motion Models

We now describe the kinematic model of the nodes. In our analysis, each node is a UAV. We consider two UAVs (UAV_1 and UAV_2) in the presence of a third UAV (UAV_J) that is trying to jam the communication link in between them. We assume that the UAVs are having a constant altitude flight. This assumption helps to simplify our analysis to a planar case. Referring to Figure 3, the configuration of each UAV in the global coordinate frame can be expressed in terms of the variables (x_i^g, y_i^g, ϕ_i^g). The subscript *i* is either 1, 2 or J depending on the UAV being referred. The pair (x_i^g, y_i^g) represents the position of a reference point on UAV_i with respect to the origin of the global reference frame and ϕ_i^g denotes the instantaneous heading of the UAV_i in the global reference frame. Hence the state space for UAV_i is $\mathbf{X}_i \cong \mathbb{R}^2 \times \text{S}^1$. In our analysis, we assume that the UAVs are a kinematic system and hence the dynamics of the UAVs are not taken into account in the differential equation governing the evolution of the system. The kinematics of the UAVs are assumed to be the following:

$$\frac{dx_i^g}{dt} = W_i \cos\phi_i^g; \frac{dy_i^g}{dt} = W_i \sin\phi_i^g; \frac{d\phi_i^g}{dt} = \sigma_i \qquad (1)$$

where, W_i and σ_i are the speed and angular velocity of UAV_i, respectively. In this paper, we assume that $\sigma_i \in [-1, +1] \quad \forall i$. Moreover, we assume that $W_i = 1 \quad \forall i$.

The state space of the entire system is $\mathbf{X}_1 \times \mathbf{X}_2 \times \mathbf{X}_j \cong \mathbb{R}^6 \times (\text{S}^1)^3$. In order to reduce the dimension of the state space we analyze the system in a coordinate frame fixed to UAV_2 as shown in Figure 3. In the new coordinate frame, the system can be modeled using six independent variables and the equations of motion of the UAV_1 and UAV_j with respect to the new coordinate frame are given by the following [13]:

$$\underbrace{\begin{pmatrix} \dot{x}_1 \\ y_1 \\ \phi_1 \\ x_j \\ y_j \\ \phi_j \end{pmatrix}}_{x} = \underbrace{\begin{pmatrix} -1+\sigma_2 y_1+\cos\phi_1 \\ -\sigma_2 x_1+\sin\phi_1 \\ -\sigma_2+\sigma_1 \\ -1+\sigma_2 y_j+\cos\phi_j \\ -\sigma_2 x_j+\sin\phi_j \\ -\sigma_2+\sigma_j \end{pmatrix}}_{f(\mathbf{x},\sigma_1.\sigma_2,\sigma_j)} \tag{2}$$

In the above expressions (x_j, y_j, ϕ_j) and (x_1, y_1, ϕ_1) represent the relative position and orientation of the UAV_j and UAV_1 in the reference frame attached to UAV_2. Hence the state space of the reduced system is isomorphic to $\mathbb{R}^4 \times (\text{S}^1)^2$.

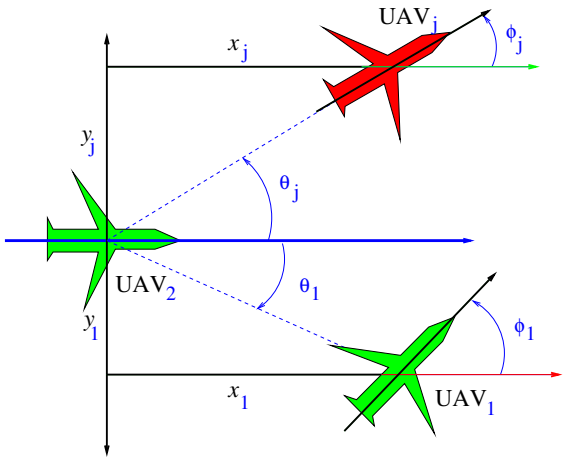

Fig. 2. Relative configuration of UAVs

C. Problem Statement

Based on the jamming model, and the motion models of the aerial vehicles, we formulate the following problem. The objective of the two aerial vehicles is to maintain an operable communication link between them, and the objective of the jammer is to break the link in finite time. Each vehicle has a complete knowledge about the state of the system. Assuming that the two UAVs can communicate in the beginning, is it possible for the jammer to disrupt the communication link in finite time?

III. Solution Technique

The jamming problem, as formulated in the previous section, is a *game of kind*. In a game of kind, the entire state space is partitioned into two disjoint regions. Although the problem considered in this paper is different from the classical capture-pursuit games that have been thoroughly studied, we borrow existing notions of capture and escape set, and introduce a slight modification in their definition to address our current scenario. We define the *capture set* as the set of initial conditions from which the jammer can disrupt the communication link in finite time. Complementary to the capture set, we define the *escape set* as the set of initial conditions of the players from which the UAVs can guarantee an operable communication link forever. The surface that separates the capture set from the escape set is called as the *barrier*. In this work, our focus is to compute the barrier, and the optimal strategies of the players on the barrier.

In [3], Isaacs studied several games of kind, and presented an elaborate description of the different kinds of barriers that might occur in such games. In this work, our specific interest lies in the construction of *natural barriers* that terminate at the boundary of the usable part [4], [1] of the terminal manifold. In the next section, we characterize the terminal surfaces for the game, and the boundary of the usable part.

IV. Termination Conditions

From the communication model, we can conclude that UAV_1 can receive messages from UAV_2 when the following condition holds:

$$\eta d(\text{UAV}_J,\text{UAV}_1) > d(\text{UAV}_1,\text{UAV}_2)$$

where $d(\text{UAV}_i,\text{UAV}_j)$ is the Euclidean distance between UAV_i and UAV_j. Similarly, UAV_2 can receive messages from UAV_1 when the following condition holds:

$$\eta d(\text{UAV}_J,\text{UAV}_2) > d(\text{UAV}_1,\text{UAV}_2)$$

Hence we can conclude that the two nodes can communicate when the following condition holds:

$$\eta \min[d(\text{UAV}_J,\text{UAV}_1), d(\text{UAV}_J,\text{UAV}_2)] > d(\text{UAV}_1,\text{UAV}_2)$$

Hence the boundary of the game set is the set of positions of the UAVs that satisfies the following condition:

$$\eta \min[d(\text{UAV}_J,\text{UAV}_1), d(\text{UAV}_J,\text{UAV}_2)] = d(\text{UAV}_1,\text{UAV}_2)$$

The set of states satisfying the above condition can be represented as the union of two smooth hypersurfaces $T_1 \bigcup T_2$, where T_1 represents the set of states in which UAV_1 does not receive any signal transmitted from UAV_2, and T_2 represents the set of states in which UAV_2 does not receive any signal transmitted from UAV_1.

For now, we will consider the set T_1, and its corresponding BUP (Boundary of Usable Part). We postpone the analysis of T_2 until Section VIII. The hypersurface T_1 is represented by the following equation in the coordinate system described in Section II:

$$\underbrace{(\sqrt{x_1^2+y_1^2} - \eta\sqrt{x_j^2+y_j^2} = 0)}_{F} \cap$$
$$((x_1-x_j)^2 + (y_1-y_j)^2 - x_j^2 + y_j^2 \geq 0) \tag{3}$$

At termination, the vector $[\dot{x}_1, \dot{y}_1, \dot{\phi}_1, \dot{x}_j, \dot{y}_j, \dot{\phi}_j]$ must penetrate the boundary of the game set on the terminal surface. In the relative coordinate system, this can be ensured only if the jammer approaches the receiver at a faster speed than the transmitter. Therefore, the usable part of the terminal manifold is given by the following condition:

$$\dot{r}_j \geq \dot{r}_1, \tag{4}$$

where $r_j = \sqrt{x_j^2 + y_j^2}$ and $r_1 = \sqrt{x_1^2 + y_1^2}$. Therefore, BUP [3] can be characterized by the following equation in addition to (15):

$$\begin{aligned} &\dot{r}_j - \dot{r}_1 = 0 \\ \Rightarrow &\frac{-x_j + x_j \cos\phi_j^* + y_j \sin\phi_j^*}{(x_j^2 + y_j^2)^{\frac{1}{2}}} - \\ &\frac{-x_1 + x_1 \cos\phi_1^* + y_1 \sin\phi_1^*}{(x_1^2 + y_1^2)^{\frac{1}{2}}} = 0 \end{aligned} \tag{5}$$

From (3), the normal to the T_1 at $(x_1, y_1, \phi_1, x_j, y_j, \phi_j)$ is given by the following expression:

$$\nu = \begin{bmatrix} \frac{\partial F}{\partial x_j} \\ \frac{\partial F}{\partial y_j} \\ \frac{\partial F}{\partial \phi_j} \\ \frac{\partial F}{\partial x_1} \\ \frac{\partial F}{\partial y_1} \\ \frac{\partial F}{\partial \phi_1} \end{bmatrix} = \begin{bmatrix} -\frac{\eta x_j}{\sqrt{x_j^2+y_j^2}} \\ -\frac{\eta y_j}{\sqrt{x_j^2+y_j^2}} \\ 0 \\ \frac{x_1}{\sqrt{x_1^2+y_1^2}} \\ \frac{y_1}{\sqrt{x_1^2+y_1^2}} \\ 0 \end{bmatrix} \tag{6}$$

V. Retrogressive path equations (RPE) for the Barrier

Based on the assumption that the barrier can be embedded in a family of semipermeable curves, the retrogressive path equations for the normals along the trajectories constituting the barrier is given by the following [3]:

$$\mathring{\nu}_k = \sum_i \nu_i \frac{\partial f_i}{\partial x_k} \quad \forall k = 1, \ldots, j, \tag{7}$$

where $\nu = [\nu_{x_1}, \nu_{y_1}, \nu_{\phi_1}, \nu_{x_j}, \nu_{y_j}, \nu_{\phi_j}]'$ represents the normal vector to the barrier. For a point on the hypersurface, there can be two normals that point in opposite directions. In this work, the normal to the barrier is chosen in the direction which points towards the capture set. From (7), we obtain the following set of differential equations for the evolution of the normal to the barrier:

$$\begin{aligned} \mathring{\nu}_{x_1} &= \sigma_2^* \nu_{y_1} \\ \mathring{\nu}_{y_1} &= -\sigma_2^* \nu_{x_1} \\ \mathring{\nu}_{\phi_1} &= \nu_{x_1} \sin\phi_1 - \nu_{y_1} \cos\phi_1 \\ \mathring{\nu}_{x_j} &= \sigma_2^* \nu_{y_j} \\ \mathring{\nu}_{y_j} &= -\sigma_2^* \nu_{x_j} \\ \mathring{\nu}_{\phi_j} &= \nu_{x_j} \sin\phi_j - \nu_{y_j} \cos\phi_j, \end{aligned}$$

where $\mathring{}$ denotes derivative with respect to retrograde time. Now we present the *regular construction* of the barrier.

VI. Strategies for the vehicles on the barrier

Based on our assumption that the barrier is embedded in a family of semipermeable surfaces, we obtain the optimal strategies of the players on the barrier. The optimal strategy for the vehicles on a semipermeable surface is governed by the following equation [3]:

$$(\sigma_1^*, \sigma_2^*, \sigma_j^*) = \arg\min_{\sigma_j} \arg\max_{\sigma_1, \sigma_2} \sum_i \nu_i f_i(\mathbf{x}, \sigma_j, \sigma_1, \sigma_2), \tag{8}$$

where ν_i represents the ith component of the vector normal to the semipermeable surface. Substituting (2) in the above equation leads to the following expression for the control law in terms of the components of the ν:

$$\begin{aligned} (\sigma_1^*, \sigma_2^*, \sigma_j^*) = \arg\min_{\sigma_j} \arg\max_{\sigma_1, \sigma_2} \sigma_2 [\nu_{x_1} y_1 - \nu_{y_1} x_1 - \nu_{\phi_1} - \\ \nu_{\phi_j} - \nu_{y_j} x_j + \nu_{x_j} y_j] + \sigma_j \nu_{\phi_j} + \sigma_1 \nu_{\phi_1} + (\nu_{x_1} \cos\phi_1 + \\ \nu_{y_1} \sin\phi_1) + (\nu_{x_j} \cos\phi_j + \nu_{y_j} \sin\phi_j) - (\nu_{x_1} + \nu_{x_j}) \end{aligned} \tag{9}$$

The above expression is separable in terms of the control of the players. Hence, the order of taking the extrema becomes inconsequential. This leads to the following expression for the optimal control of the individual aerial vehicles.

$$\begin{aligned} \sigma_2^* = \text{sign}[\nu_{x_1} y_1 - \nu_{y_1} x_1 - \nu_{\phi_1} - \nu_{\phi_j} - \nu_{y_j} x_j + \nu_{x_j} y_j] \\ \sigma_j^* = -\text{sign}(\nu_{\phi_j}) \\ \sigma_1^* = \text{sign}(\nu_{\phi_1}) \end{aligned} \tag{10}$$

The above expressions provide the optimal control of the vehicles in terms of the normal to the barrier. From the RPE, we can compute the evolution of the normal in terms of the optimal control of the vehicles.

VII. Optimal Controls and Initial Conditions

From (10), we can conclude that the controls are uniquely defined only if the argument of the sign function is non-zero. Singularity in the controls arises when the aforementioned condition is not satisfied. These are states in which the value of the control does the effect the minimization or maximization of (9). Such a situation arises at the terminal manifold. This leads to an ill-conditioned boundary condition for the RPE which must be integrated in retrograde time for the construction of the barrier. In order to resolve this problem, we analyze the higher order derivatives of the arguments of the sign function.

Theorem 1: At termination on the BUP, the optimal control of the vehicles is given by the following expression:

$$\sigma_1^* = \begin{cases} 1 & 0 < (\theta_1^f - \phi_1^f) < \pi \\ -1 & \pi < (\theta_1^f - \phi_1^f) < 2\pi \\ 0 & |\theta_1^f - \phi_1^f| = \pi \\ \{+1, -1\} & \theta_1^f = \phi_1^f \end{cases}$$

$$\sigma_j^* = \begin{cases} -1 & 0 < (\theta_j^f - \phi_j^f) < \pi \\ 1 & \pi < (\theta_j^f - \phi_j^f) < 2\pi \\ \{+1, -1\} & |\theta_j^f - \phi_j^f| = \pi \\ 0 & \theta_j^f = \phi_j^f \end{cases}$$

$$\sigma_2^* = \begin{cases} 1 & \frac{2\sin(\phi_1^f - \theta_1^f) + \cos\theta_1^f}{2\sin(\phi_j^f - \theta_j^f) + \cos\theta_j^f} < \eta \\ -1 & \text{otherwise} \end{cases}$$

Proof: In order to compute the terminal value of the controls, we compute the higher order derivatives of the

arguments in the sign function in (10). This leads to the following:

1) σ_1:

$$\sigma_1^* = \text{sign}A,$$

where $A = \nu_{\phi_1}$.

$$\begin{aligned} \mathring{A} &= \nu_{x_1}\sin\phi_1 - \nu_{y_1}\cos\phi_1 \\ \frac{d^2A}{d\tau^2} &= (\nu_{y_1}\sin\phi_1 + \nu_{x_1}\cos\phi_1)\underbrace{(\sigma_2^* + \mathring{\phi}_1)}_{\sigma_1^*} \end{aligned}$$

At termination, we obtain the following expressions for the higher derivatives:

$$\begin{aligned} \mathring{A}|_{\tau=0} &= \sin(\theta_1^f - \phi_1^f) \\ \frac{d^2A}{d\tau^2}|_{\tau=0} &= \cos(\theta_1^f - \phi_1^f)\sigma_1^*(0) \end{aligned} \quad (11)$$

2) σ_j:

$$\sigma_j^* = -\text{sign}A,$$

where $A = \nu_{\phi_j}$.

$$\begin{aligned} \mathring{A} &= \nu_{x_j}\sin\phi_j - \nu_{y_j}\cos\phi_j \\ \frac{d^2A}{d\tau^2} &= (\nu_{y_j}\sin\phi_j + \nu_{x_j}\cos\phi_j)\underbrace{(\sigma_2^* + \mathring{\phi}_1)}_{\sigma_j^*} \end{aligned}$$

At termination, we obtain the following expressions for the higher derivatives:

$$\mathring{A}|_{\tau=0} = \sin(\theta_j^f - \phi_j^f), \quad \frac{d^2A}{d\tau^2}|_{\tau=0} = \cos(\theta_j^f - \phi_j^f)\sigma_j^*(0)$$

3) σ_2:

$$\sigma_2^* = \text{sign}A,$$

where

$$A = \nu_{x_1}y_1 - \nu_{y_1}x_1 - \nu_{\phi_1} - \nu_{\phi_j} - \nu_{y_j}x_j + \nu_{x_j}y_j$$

$$\begin{aligned} \frac{dA}{d\tau} = 2\sigma_2^*[\nu_{x_1}x_1 + \nu_{y_1}y_1 + \nu_{y_j}y_j + \nu_{x_j}x_j] - 2[\nu_{x_1}\sin\phi_1 \\ -\nu_{y_1}\cos\phi_1 - \nu_{y_j}\cos\phi_j + \nu_{x_j}\sin\phi_j] - (\nu_{y_1} + \nu_{y_j}) \end{aligned}$$

At termination, we obtain the following values of the higher derivatives:

$$\begin{aligned} \frac{dA}{d\tau}|_{\tau=0} = -2[\sin(\phi_1 - \theta_1) - \eta\sin(\phi_j - \theta_j)] - \\ (\cos\theta_1 - \eta\cos\theta_j) \end{aligned}$$

Let us consider σ_1^*. From (11), we can conclude that if $\nu_{\phi_1}|_{\tau=0} = 0$, $\text{sign}(\nu_{\phi_1}|_{\tau=0^+}) = \text{sign}(\sin(\theta_1^f - \phi_1^f))$. If $\sin(\theta_1^f - \phi_1^f) \neq 0$, then the value of σ_1^* is well defined just before termination. Now let us consider the case when $\sin(\theta_1^f - \phi_1^f) = 0$. In that case, $\cos(\theta_1^f - \phi_1^f) \neq 0$, and we can consider the term $\frac{d^2A}{d\tau^2}$. If $\cos(\theta_1^f - \phi_1^f) > 0 \Rightarrow \sigma_1^*(0^-) = \text{sign}(\sigma_1^*(0^-))$. On the other hand, if $\cos(\theta_1^f - \phi_1^f) < 0 \Rightarrow \sigma_1^*(0^-) = \text{sign}(-\sigma_1^*(0^-)) \Rightarrow \sigma_1^*(0^-) = 0$.

In a similar manner, we can derive the expression for the control law for the remaining vehicles at termination. ■

Now we derive closed form expression for the trajectories of the vehicles. In order to do so, we consider an interval of time $[\tau_0, \tau_f]$ such that σ_1^*, σ_2^* and σ_j^* are uniquely defined from their arguments, and their values are constant throughout the interval. From the RPE for the component of the normal corresponding to UAV_1, we obtain the following relation:

$$\frac{d^2\nu_{x_1}}{d\tau^2} = -(\sigma_2^*)^2\nu_{x_1}$$

The solution to the above differential equation is given by the following:

$$\nu_{x_1}(\tau) = a_{x_1}\sin(\sigma_2^*(\tau - \tau_0)) + b_{x_1}\cos(\sigma_2^*(\tau - \tau_0)), \quad (12)$$

where $a_{x_1} = \nu_{y_1}(\tau_0)$ and $b_{x_1} = \nu_{x_1}(\tau_0)$. Substituting the value of ν_{x_1} into the RPE for ν_{y_1}, we obtain the following expression of $\nu_{y_1}(\tau)$:

$$\nu_{y_1}(\tau) = a_{x_1}\cos(\sigma_2^*(\tau - \tau_0)) - b_{x_1}\sin(\sigma_2^*(\tau - \tau_0)) \quad (13)$$

From (12) and (13), we obtain the following expression:

$$\mathring{\nu}_{\phi_1} = b_{x_1}\sin(g(\tau)) - a_{x_1}\cos(g(\tau)),$$

where $g(\tau) = \sigma_1^*(\tau - \tau_0) + \phi_1(\tau)$.

$$\Rightarrow \nu_{\phi_1}(\tau) = \nu_{\phi_1}(\tau_0) + \frac{-1}{\sigma_1^*}[a_{x_1}\sin(g(\tau)) + b_{x_1}\cos(g(\tau))] \quad (14)$$

In a similar manner, we obtain the following expressions for the remaining components of the normal:

$$\begin{aligned} \nu_{x_j}(\tau) &= \nu_{x_j}(\tau_0) + a_{x_j}\sin(\sigma_2^*(\tau - \tau_0)) + \\ & b_{x_j}\cos(\sigma_2^*(\tau - \tau_0)) \\ \nu_{y_j}(\tau) &= \nu_{y_j}(\tau_0) + a_{x_j}\cos(\sigma_2^*(\tau - \tau_0)) - \\ & b_{x_j}\sin(\sigma_2^*(\tau - \tau_0)) \\ \nu_{\phi_j}(\tau) &= \nu_{\phi_j}(\tau_0) + \frac{-1}{\sigma_j^*}[a_{x_j}\sin(g(\tau)) + \\ & b_{x_j}\cos(g(\tau))], \end{aligned}$$

where $a_{x_j} = \nu_{y_j}(\tau_0)$ and $b_{x_j} = \nu_{x_j}(\tau_0)$.

VIII. Termination Surface T_2

Now we describe the construction of the barrier emanating from terminal surface T_2.

$$\underbrace{(\sqrt{x_1^2 + y_1^2} - \eta\sqrt{(x_1 - x_j)^2 + (y_1 - y_j)^2} = 0)}_{F} \cap$$
$$((x_1 - x_j)^2 + (y_1 - y_j)^2 - (x_1^2 + y_1^2) \geq 0) \quad (15)$$

The usable part of the terminal manifold is characterized by the fact that the jammer approaches UAV_2 at a rate faster than UAV_1. Therefore, the boundary of the usable part on T_2 is characterized by the following equation:

$$\begin{aligned} \frac{(x_1 - x_j)(\dot{x}_1 - \dot{x}_j) + (y_1 - y_j)(\dot{y}_1 - \dot{y}_j)}{\sqrt{(x_1 - x_j)^2 + (y_1 - y_j)^2}} = \\ \frac{-x_1 + x_1\cos\phi_1^* + y_1\sin\phi_1^*}{\sqrt{x_1^2 + y_1^2}} \end{aligned} \quad (16)$$

The normal to the terminal manifold is given by the following vector:

$$\nu = \begin{bmatrix} \frac{\partial F}{\partial x_j} \\ \frac{\partial F}{\partial y_j} \\ \frac{\partial F}{\partial \phi_j} \\ \frac{\partial F}{\partial x_1} \\ \frac{\partial F}{\partial y_1} \\ \frac{\partial F}{\partial \phi_1} \end{bmatrix} = \begin{bmatrix} \frac{\eta x_j}{\sqrt{(x_1-x_j)^2+(y_1-y_j)^2}} \\ \frac{\eta y_j}{\sqrt{(x_1-x_j)^2+(y_1-y_j)^2}} \\ 0 \\ \frac{x_1}{\sqrt{x_1^2+y_1^2}} - \frac{\eta x_1}{\sqrt{(x_1-x_j)^2+(y_1-y_j)^2}} \\ \frac{y_1}{\sqrt{x_1^2+y_1^2}} - \frac{\eta y_1}{\sqrt{(x_1-x_j)^2+(y_1-y_j)^2}} \\ 0 \end{bmatrix} \quad (17)$$

The optimal controls of the players on the barrier is given by (10). The RPE for the normal to the barrier remain unchanged. The boundary conditions to the RPE can be obtained in the same manner as in Section VII.

Theorem 2: At termination on the BUP, the optimal control of the vehicles is given by the following expression:

$$\sigma_1^* = \begin{cases} \text{sign}(\eta-1) & 0 < (\theta_1^f - \phi_1^f) < \pi \\ -\text{sign}(\eta-1) & \pi < (\theta_1^f - \phi_1^f) < 2\pi \\ 0 & |\theta_1^f - \phi_1^f| = \pi, \eta < 1 \\ \{+1,-1\} & \theta_1^f = \phi_1^f, \eta < 1 \\ \{+1,-1\} & |\theta_1^f - \phi_1^f| = \pi, \eta > 1 \\ 0 & \theta_1^f = \phi_1^f, \eta > 1 \end{cases}$$

$$\sigma_j^* = \begin{cases} -1 & 0 < (\theta_j^f - \phi_j^f) < \pi \\ 1 & \pi < (\theta_j^f - \phi_j^f) < 2\pi \\ \{+1,-1\} & |\theta_j^f - \phi_j^f| = \pi \\ 0 & \theta_j^f = \phi_j^f \end{cases}$$

$$\sigma_2^* = \begin{cases} \pm 1 & a > b, a+b > 0 \\ \{-1,0\} & a < b, a+b > 0 \\ \{1,0\} & a > b, a+b < 0 \\ 0 & a < b, a+b < 0 \end{cases}$$

where

$$\begin{aligned} a &= [(1-\eta^2)\sqrt{x_1^2+y_1^2} + \gamma\eta\sqrt{x_j^2+y_j^2}] \\ b &= 2[(1-\eta^2)\sin(\phi_1-\theta_1) - \eta\gamma\sin(\phi_j-\theta_j)] - \\ &\quad (1-\eta^2)\cos\theta_1 - \eta\gamma\cos\theta_j \end{aligned}$$

Proof: In order to compute the terminal value of the controls, we compute the higher order derivatives of the arguments in the sign function in (10). This leads to the following:

1) σ_1:

$$\sigma_1^* = \text{sign}A,$$

where $A = \nu_{\phi_1}$.

$$\begin{aligned} \mathring{A} &= \nu_{x_1}\sin\phi_1 - \nu_{y_1}\cos\phi_1 \\ \frac{d^2A}{d\tau^2} &= (1-\eta^2)(\nu_{y_1}\sin\phi_1 + \nu_{x_1}\cos\phi_1)\underbrace{(\sigma_2^* + \mathring{\phi}_1)}_{\sigma_1^*} \end{aligned}$$

At termination, we obtain the following expressions for the higher derivatives:

$$\begin{aligned} \mathring{A}|_{\tau=0} &= (1-\eta^2)\sin(\theta_1^f - \phi_1^f) \\ \frac{d^2A}{d\tau^2}|_{\tau=0} &= (1-\eta^2)\cos(\theta_1^f - \phi_1^f)\sigma_1^*(0) \end{aligned}$$

2) σ_j:

$$\sigma_j^* = -\text{sign}A,$$

where $A = \nu_{\phi_j}$.

$$\begin{aligned} \mathring{A} &= \nu_{x_j}\sin\phi_j - \nu_{y_j}\cos\phi_j \\ \frac{d^2A}{d\tau^2} &= (\nu_{y_j}\sin\phi_j + \nu_{x_j}\cos\phi_j)\underbrace{(\sigma_2^* + \mathring{\phi}_1)}_{\sigma_j^*} \end{aligned}$$

At termination, we obtain the following expressions for the higher derivatives:

$$\begin{aligned} \mathring{A}|_{\tau=0} &= \gamma\sin(\theta_j^f - \phi_j^f) \\ \frac{d^2A}{d\tau^2}|_{\tau=0} &= \gamma\cos(\theta_j^f - \phi_j^f)\sigma_j^*(0), \end{aligned}$$

where $\gamma = \frac{\sqrt{x_j^2+y_j^2}}{\sqrt{(x_1-x_j)^2+(y_1-y_j)^2}}$

3) σ_2:

$$\sigma_2^* = \text{sign}A,$$

where

$$A = \nu_{x_1}y_1 - \nu_{y_1}x_1 - \nu_{\phi_1} - \nu_{\phi_j} - \nu_{y_j}x_j + \nu_{x_j}y_j$$

$$\begin{aligned} \frac{dA}{d\tau} = 2\sigma_2^*[\nu_{x_1}x_1 + \nu_{y_1}y_1 + \nu_{y_j}y_j + \nu_{x_j}x_j] - \\ 2[\nu_{x_1}\sin\phi_1 - \nu_{y_1}\cos\phi_1 - \\ \nu_{y_j}\cos\phi_j + \nu_{x_j}\sin\phi_j] - (\nu_{y_1} + \nu_{y_j}) \end{aligned}$$

$$\begin{aligned} \frac{dA}{d\tau}|_{\tau=0} = 2\sigma_2^*[(1-\eta^2)\sqrt{x_1^2+y_1^2} + \gamma\eta\sqrt{x_j^2+y_j^2}] - \\ 2[(1-\eta^2)\sin(\phi_1-\theta_1) - \eta\gamma\sin(\phi_j-\theta_j)] - \\ (1-\eta^2)\cos\theta_1 - \eta\gamma\cos\theta_j \end{aligned}$$

From arguments similar to the proof of Theorem 1, we obtain all possible values of control at termination as given in the statement of the theorem. ∎

Since the RPE remains unchanged, trajectories of the vehicles once they are on the barrier, and have constant controls have the same form as presented in the previous section.

IX. Results

In this section, we present the simulation results for the trajectories of the vehicles in the reference frame of UAV_2 when the state of the system is on the barrier. In Figure 3, UAV_2 is represented by the green circle at the origin. The red and blue circle represent the position of UAV_1 and the jammer, respectively, at the BUP of T_1. The value of $\eta = 0.5$. The red and the blue curves show the trajectories of UAV_1 and the jammer, respectively, for 3000 sec on the barrier just before the vehicles reach the BUP. Figure 4 shows the trajectories of the vehicles for termination on BUP of T_2. Similarly, figures 5 and 6 show the trajectory and control of the vehicles on the barrier prior to termination on the BUP of T_1 and T_2, respectively, for $\eta = 1.5$. All the simulations show a lot of chattering in the controls of UAV_2.

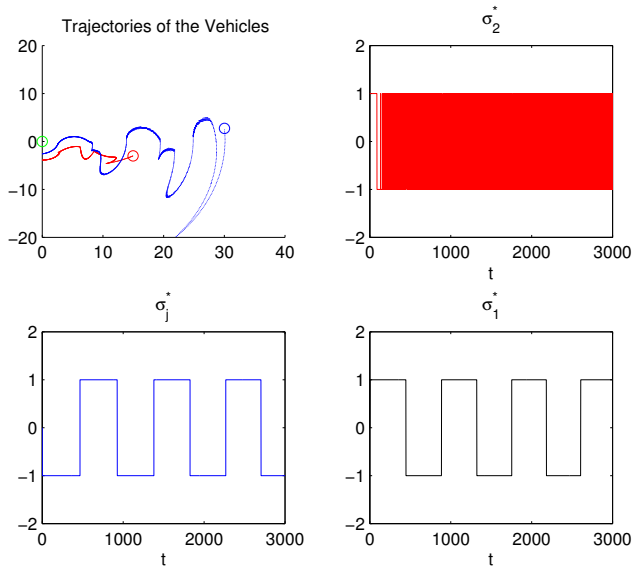

Fig. 3. Trajectories and controls of UAV_1 and the jammer

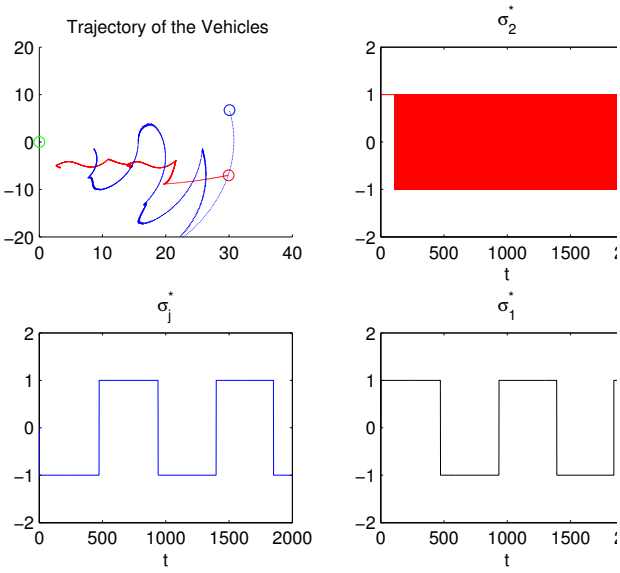

Fig. 4. Trajectories and controls of UAV_1 and the jammer

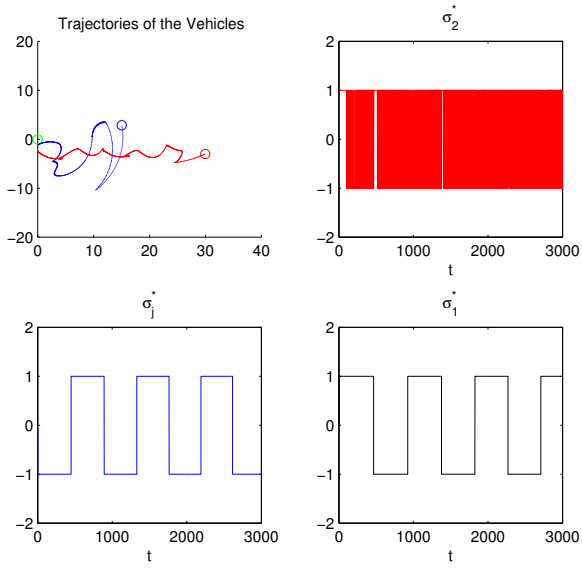

Fig. 5. Trajectories and controls of UAV_1 and the jammer

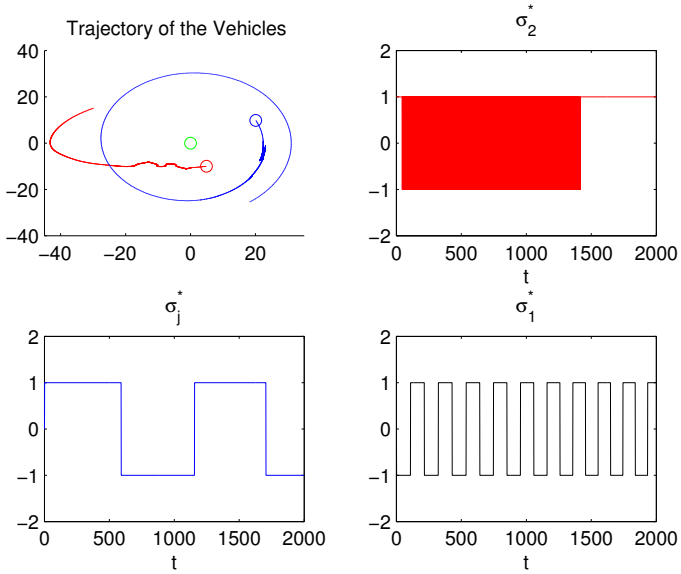

Fig. 6. Trajectories and controls of UAV_1 and the jammer

X. Conclusion

In this work, we analyzed an intrusion-evasion game involving two UAVs and a jammer. The scenario was modeled as a game of kind. The central focus was the construction of the natural barriers emanating from the BUP of the terminal manifold, and the optimal control of the vehicles on the barrier. Simulation results were depicted for specific termination conditions for two different values of the physical parameters of the problem (η). Future work involves the computation of the intersection of the barriers from the two terminal manifolds, and subsequent termination of further construction. This will divide the entire state space into the escape and the capture set.

References

[1] T. Başar and G. J. Olsder. *Dynamic Noncooperative Game Theory, 2nd Ed.* SIAM Series in Classics in Applied Mathematics, Philadelphia, 1999.

[2] S. Bhattacharya and T. Başar. Game-theoretic analysis of an aerial jamming attack on a UAV communication network. In *Proceedings of American Control Conference*, pages 818–823, Baltimore, Maryland, June 2010.

[3] R. Isaacs. *Differential Games*. Wiley, New York, 1965.

[4] J. Lewin. *Differential Games: Theory and Methods for Solving Game Problems with Singular Surfaces*. Springer-Verlag, London, 1994.

[5] J. Lewin and G. J. Olsder. Conic surveillance evasion. *Journal of Optimization Theory and Applications*, 27(1):339–353, 1979.

[6] A. W. Merz. The game of two identical cars. *Journal of Optimization Theory and Applications*, 9(5):324–343, 1972.
[7] G. Noubir and G. Lin. Low power denial of service attacks in data wireless lans and countermeasures. 2003.
[8] P. Papadimitratos and Z. J. Haas. Secure routing for mobile ad hoc networks. January 2002.
[9] V. S. Patsko and V. L. Turova. Semipermeable curves and level sets of value function in differential games with the Homicidal Chauffer Dynamics. In *Optimal control of complex structures*, pages 191–202. Birkhauser.
[10] V. S. Patsko and V. L. Turova. Families of semipermeable curves in differential games with homicidal chauffer dynamics. *Automatica*, 40(12):2059–2068, 2004.
[11] R. A. Poisel. *Modern Communication Jamming Principles and Techniques*. Artech, Massachussets, 2004.
[12] J. J. Proakis and M. Salehi. *Digital Communications*. McGraw-Hill, 2007.
[13] S. Shankaran, D. Stipanović, and C. Tomlin. Collision avoidance strategies for a three player game. In *International Society of Dynamic Games*, Wroclaw, Poland, July 2008.